

# Quantum Monte Carlo calculations of the structural properties and the B1-B2 phase transition of MgO

D. Alfè<sup>1,2</sup>, M. Alfredsson<sup>1</sup>, J. Brodholt<sup>1</sup> and M. J. Gillan<sup>2</sup>

<sup>1</sup>Department of Earth Sciences, University College London  
Gower Street, London WC1E 6BT, UK

<sup>2</sup>Department of Physics and Astronomy, University College London  
Gower Street, London WC1E 6BT, UK

M. D. Towler and R. J. Needs

Theory of Condensed Matter Group, Cavendish Laboratory, University of Cambridge  
Cambridge CB3 0HE, UK

October 4, 2018

## Abstract

We report diffusion Monte Carlo (DMC) calculations on MgO in the rock-salt and CsCl structures. The calculations are based on Hartree-Fock pseudopotentials, with the single-particle orbitals entering the correlated wave function being represented by a systematically convergeable cubic-spline basis. Systematic tests are presented on system-size errors using periodically repeating cells of up to over 600 atoms. The equilibrium lattice parameter of the rock-salt structure obtained within DMC is almost identical to the Hartree-Fock result, which is close to the experimental value. The DMC result for the bulk modulus is also in good agreement with the experimental value. The B1-B2 transition pressure (between the rock-salt and CsCl structures) is predicted to be just below 600 GPa, which is beyond the experimentally accessible range, in accord with other predictions based on Hartree-Fock and density functional theories.

## 1 Introduction

The quantum Monte Carlo (QMC) technique is becoming an increasingly important tool in the study of condensed matter [1]. Competitive in accuracy with high-level quantum chemistry methods, it has the enormous advantage of being practicable for large systems containing hundreds of atoms. The power of QMC in overcoming the deficiencies of density functional theory (DFT) has been amply demonstrated by recent applications, including the energetics of point defects in silicon [2] and carbon [3], the reconstruction of the Si (001) surface [4] and its interaction with H<sub>2</sub> [5], and the calculation of optical excitation energies [6]. Nevertheless, the classes of materials to which QMC has been applied have so far been rather limited. Oxide materials are likely to be a very fruitful field for the application of QMC, but in exploring this field it is clearly important to study the capabilities of the techniques for the simplest possible oxides. We present here QMC calculations on MgO, focusing on its elementary bulk properties, including the equilibrium lattice parameter of the rock-salt structure, the stable structure under ambient conditions, and the pressure of the B1-B2 transition between the rock-salt and CsCl structures.

Two types of QMC are relevant here. In the first, known as variational Monte Carlo (VMC), a trial many-electron wave function is constructed as the product of a Slater determinant of single-electron orbitals and the so-called Jastrow correlation factor. The latter is parameterised, and the parameter values are obtained using a stochastic optimisation procedure. Since VMC by itself is not usually accurate enough, the optimised many-electron wave function produced by VMC is then used in diffusion Monte Carlo (DMC) [1, 7], which improves the ground-state estimate by performing an evolution in imaginary time. In

principle, the ground-state energy would be exact, but to overcome the fermion sign problem we use the standard “fixed-node approximation” [8]. In practice, only the valence electrons are treated explicitly, the interactions between the valence and core electrons being represented by pseudopotentials. This introduces additional approximations, including the “pseudopotential locality approximation”. The calculations are performed on periodically repeated cells, and system size errors need to be carefully treated. However, in many cases, the overall errors within QMC can be made much smaller than those within DFT, and QMC has already been important in revealing, quantifying and overcoming DFT errors in such quantities as defect formation energies, surface reaction energies and energy barriers [2, 3, 5].

The three main purposes of this work are: first, to establish the technical feasibility of performing QMC on MgO; second, to study differences between DFT and QMC predictions for the properties of bulk MgO; and third, to prepare the way for QMC work on more challenging oxides. As one of the simplest oxides, MgO has often been used as a paradigm for testing theoretical techniques. For QMC, the issue of technical feasibility is a non-trivial one, since the computing effort required to obtain accurate results with DMC depends heavily on the ability of VMC to deliver wave functions which are sufficiently close to the exact ground-state wave function. If sufficiently accurate trial wave functions cannot be obtained, the DMC calculations may even become unstable. The electronic simplicity of MgO is expected to ease the task of finding good trial wave functions.

The concerns of this work are not purely technical. The pressure-induced transition from the rock-salt to CsCl structure in MgO has been much studied because of its geological interest (see, e.g., [9, 10] and references therein). We also expect that the present work will provide the basis for applying QMC to several important and controversial questions related to ionic materials such as MgO, including the adsorption and dissociation of molecules on their surfaces (see, e.g., Ref. [11]), the self-trapping of hole centres and their trapping at defects (see, e.g., Ref. [12]), and the conflict between theory and experiment for the slope,  $dT/dp$ , of their melting curves [13, 14, 15, 16]. Beyond this, we hope that the experience gained here will help to prepare the way for the application of QMC to transition-metal oxides such as FeO, where electron correlation is highly non-trivial. DMC studies of NiO [17] and MnO [18] have already shown the feasibility of calculations on these materials, but those studies did not include energy-volume curves, and the unit cells used were not large enough to give the accuracy required here.

In the following Section we summarise the QMC techniques used here. In Sec. 3, we present tests on the magnitude of various errors, including system-size errors, and we report our results for the total energy as a function of volume for the rock-salt and CsCl structures, and the transition pressure between the two. Discussion, prospects for future work, and conclusions are presented in Sec. 4.

## 2 Techniques

Detailed descriptions of VMC and DMC have already been reported [1], so here we only outline rather briefly the main features of the present work. All the QMC calculations presented here were performed using the CASINO code, the technical details of which are given in Ref. [19].

Our trial wave functions are of the Slater-Jastrow type:

$$\Psi_T(\mathbf{R}) = D^\uparrow D^\downarrow e^J, \quad (1)$$

where  $D^\uparrow$  and  $D^\downarrow$  are Slater determinants of up- and down-spin single-electron orbitals, and  $e^J$  is the so-called Jastrow factor, describing the correlation between the electrons. We use single-electron orbitals obtained from DFT calculations. These single-particle orbitals fix the nodal surface (the surface in configuration space on which the wave function vanishes and across which it changes sign). Within this “fixed-node approximation” DMC gives a variational upper bound to the ground state energy, rather than the exact ground state energy. However, because of its large band-gap, we expect that a single Slater determinant will give a good description of the nodal surface of MgO. The function  $J$  appearing in the Jastrow factor is a sum of parametrized one-body and two-body terms [20], the latter being designed to satisfy the cusp conditions. The free parameters in  $J$  are determined by requiring that the variance of the local energy in VMC be as small as possible [21, 22].

In the present work, the many-body wave function represents explicitly only valence electrons, whose interactions with the ionic cores are represented by pseudopotentials. We used pseudopotentials generated within Hartree-Fock (HF) theory, but including scalar relativistic effects [23]. There is evidence to show that HF theory provides better pseudopotentials for use within QMC than DFT [24]. The core radii of our pseudopotentials are  $r(\text{O}2s) = 0.423 \text{ \AA}$ ,  $r(\text{O}2p) = 0.397 \text{ \AA}$ ,  $r(\text{O}3d) = 0.524 \text{ \AA}$ ,  $r(\text{Mg}3s) = r(\text{Mg}3p) = r(\text{Mg}3d) = 1.259 \text{ \AA}$ .

The single-particle orbitals entering the Slater determinants of Eq. (1) are the most important component of the wave function. Filippi and Fahy [32] have developed a method for optimising orbitals within VMC, which achieved an energy reduction in diamond from optimising LDA orbitals of 0.040(16) eV per atom. Kent *et al.* [25] found that in bulk silicon using LDA orbitals in a VMC calculation gave an energy 0.024(4) eV per atom lower than HF orbitals. These energy changes would be significantly reduced in DMC and it appears that HF and LDA orbitals are sufficient for these systems. In this work we have used LDA orbitals obtained using the plane-wave pseudopotential DFT code PWSCF [26].

The basis set used to represent the single-particle orbitals in the QMC calculations themselves is not plane-waves, which become very inefficient for large systems, because the computation cost of evaluating an orbital is proportional to the system size. Instead, we use a B-spline basis, also known as blip functions, consisting of piecewise continuous localised cubic spline functions centred on a regular grid of points. A detailed explanation of blip functions, and their great advantages for QMC calculations has been reported elsewhere [27]. The blip basis is closely related to a plane-wave basis, and for a plane-wave cut-off energy  $E_{\text{cut}} = \hbar^2 k_{\text{cut}}^2 / 2m$  ( $m$  is the electron mass), there is a natural choice of blip-grid spacing  $a$  given by  $a = \pi / k_{\text{cut}}$ . In the same way that plane-wave convergence is achieved by increasing  $k_{\text{cut}}$ , blip convergence is achieved by reducing  $a$ . Because of the relationship between plane-waves and blips, it is straightforward to transform the plane-wave coefficients from the PWSCF calculations into the blip coefficients needed for the QMC calculations, as explained in more detail in our earlier paper [27].

For QMC calculations on perfect crystals, there is a useful device which allows a considerable saving of memory. Instead of constructing single-particle orbitals at a given  $\mathbf{k}$ -point (e.g., the  $\Gamma$  point) for the large repeating cell, we construct them for the primitive cell at the corresponding set of  $\mathbf{k}$ -points. The plane wave coefficients from this calculation are then converted to blip coefficients on points of the blip-grid within the primitive cell. At run-time, a simple conversion allows these stored coefficients to be used to calculate the required values of the single-particle orbitals at any point in the large repeating cell. The key point here is that it is unnecessary to store blip coefficients at grid points covering the entire large repeating cell.

An important source of error in QMC calculations using periodic boundary conditions is the limited size of the repeating cell, and the convergence of the QMC energy with respect to the size of the simulation cell must be carefully investigated. To improve this convergence, we follow the common practice [33] of correcting for this error by using separate DFT calculations: we add to the DMC energies the difference  $\Delta E_{\Gamma \rightarrow \mathbf{k}}$  between the DFT-LDA energy calculated with a very large set of  $\mathbf{k}$ -points and the DFT-LDA energy calculated using the same sampling as in the DMC calculation. The question of correcting for finite size errors in the Coulomb energy has been addressed in recent papers [28, 29, 30], and a method known as the model periodic Coulomb (MPC) interaction has been developed. The finite size error in the Ewald interaction energy arises from the exchange-correlation energy, which can be written as the interaction of the electrons with their exchange-correlation holes. The interaction with the hole should have the standard  $1/r$  form, but within periodic boundary conditions this must be replaced by a periodic interaction. The MPC interaction maintains the correct Ewald interaction for evaluating the Hartree energy while for the exchange-correlation energy a periodically repeated potential based on the  $1/r$  form is used. This significantly reduces the finite size errors in the interaction energy, although effects due to the squeezing of the exchange-correlation hole into a finite cell still remain.

We also mention two other technical points relating to size effects. DMC calculations require the use of real trial wave functions. However, these can be constructed using single-particle orbitals obtained either from calculations at the  $\Gamma$ -point or, in general,  $\mathbf{k}$ -points which correspond to one half of a reciprocal lattice vector of the simulation cell [31]. The difference between QMC energies obtained in these two ways can be used as an indication of the system size errors. The other point is that a given physical crystal structure

can be treated using large repeating cells associated with different Bravais lattices. Since MgO in both the rock-salt and CsCl structures has cubic symmetry, it is most natural to use Bravais lattices for the repeating cell having simple-cubic (sc), body-centred-cubic (bcc) or face-centred-cubic (fcc) symmetries. We expect that the fcc repeating geometry will give the best convergence with respect to system size, and we shall present results which illustrate this effect.

The number of walkers in DMC simulations is governed by a population control algorithm, which has the purpose of maintaining this number roughly constant. In order to minimise statistical bias in the total energy, the calculations need to be run with a large population of walkers. For our DMC calculations we have used a target population of 640 walkers, which also makes it efficient to run on massively parallel machines, with parallelism achieved by distributing walkers across processors. For the imaginary time evolution of the walkers we found that a time step of 0.005 a.u. gave time step errors in the DMC energy of less than 10 meV/atom.

## 3 Results

### 3.1 Technical tests

We have found that the quality of our Slater-Jastrow trial wave function is improved if a large plane-wave cut-off is used in generating the single-particle orbitals, and a correspondingly small blip-grid spacing is used in representing them. In order to investigate this question, we performed a series of VMC calculations, and calculated the standard error in the energy as a function of plane-wave cut-off. The blip-grid spacing was taken to be related to the plane-wave cut-off by the ‘natural’ formula mentioned in Sec. 2. The calculations were performed without a Jastrow factor, because this makes it possible to check some components of the total energy against DFT calculations. These calculations were performed on a 16-atom cell for MgO in the rock-salt structure with a lattice parameter of  $a = 4.17 \text{ \AA}$ , which is close to the zero pressure equilibrium lattice parameter. Results are presented in Fig. 1. We notice that by increasing the PW cutoff from 680 eV to 6800 eV the standard error in the energy is reduced by a factor of  $\sim 2$ . This means that QMC runs performed using the trial wave function obtained with the largest cutoff can be 4 times shorter, in order to achieve the same statistical accuracy. More importantly, we found that using a very large PW cutoff was essential for having stable DMC runs. We were unable to perform any useful DMC simulation with cutoff energies less than 2712 eV.

We have made extensive tests on system size effects. We divide our discussion of these tests into two parts: first, tests on the rock-salt structure at low pressures, which are relevant to the equilibrium properties of this structure; second, tests on both the rock-salt and CsCl structures at high pressures, which are relevant to the determination of the transition pressure. As we shall see, these two sets of tests involve somewhat different questions. In Fig. 2, we show the VMC energy per atom of MgO as a function of the number of atoms in the repeating cell, using both the standard Ewald interaction and the MPC interaction. For these calculations we used a plane-wave cut-off of 6800 eV and the associated natural blip-grid spacing for the description of the single-particle orbitals. We note that the MPC results appear to converge considerably faster than the Ewald ones, and that for a system of 54 atoms the MPC energy is already converged to better than  $\sim 50 \text{ meV/atom}$ . We therefore decided to use this cell size to evaluate the energy-volume curve presented in the following section.

The results we report here for the CsCl structure were performed with the standard Ewald method rather than the MPC method. In order to check system-size errors thoroughly, we found it essential to perform tests on large systems of up to over 600 atoms. We made extensive tests on the CsCl structure to compare sc and fcc repeating geometries and to examine the effect of using different sampling wavevectors. The sampling wavevectors we used are the  $\Gamma$ -point  $(2\pi/L)(0, 0, 0)$ , and the wavevector  $(2\pi/L)(0.5, 0.5, 0.5)$ , where  $L$  specifies the dimension of the repeated cell. (In more detail,  $L$  is the length such that with sc repeating geometry the primitive translation vectors are  $L(1, 0, 0)$ ,  $L(0, 1, 0)$  and  $L(0, 0, 1)$ , while with fcc geometry they are  $L(0, 0.5, 0.5)$ ,  $L(0.5, 0, 0.5)$  and  $L(0.5, 0.5, 0)$ .) Since the wavevector  $(2\pi/L)(0.5, 0.5, 0.5)$  lies on the zone boundary of the Brillouin zone associated with the periodically repeated supercell, we refer to sampling using this wavevector as “zone-boundary” sampling. These tests were performed at the

volume  $8.77 \text{ \AA}^3/\text{atom}$ , which is close to the zero pressure equilibrium volume. The tests were all performed using VMC, and we used the Jastrow factor optimised using a 16 atom cell for all system sizes, because re-optimising the Jastrow factor introduces small “jumps” in the energy. Since we needed to go to large system sizes, we decided to reduce the plane-wave cut-off from 6800 eV to 2712 eV, because this gave a considerable reduction in the memory required; with this lower cut-off, the standard error in the energy fluctuations is only slightly larger (see Fig. 1), and DMC calculations are still stable. Results of these tests are shown in Fig. 3. We see that convergence to within less than 50 meV/atom is obtained for systems larger than 108/128 atom. We also note that convergence is better with the fcc than with the sc repeating geometry, as expected, and that there is little to choose between  $\Gamma$ -point and “zone-boundary” sampling. We have therefore performed all further calculations using fcc geometry and  $\Gamma$ -point sampling.

Since calculation of the transition pressure requires QMC calculations for the two structures at high pressures, we have performed further VMC calculations at volumes 4.23 and 4.41  $\text{\AA}^3/\text{atom}$  for the CsCl and the rock-salt structures respectively, close to the transition, using the Ewald interaction. Results of these tests are reported in Table 2. We see that for calculations on the CsCl structure, using a cell containing 108 atoms with fcc repeating geometry, the error is about 50 meV/atom. The error is approximately the same for the rock-salt structure with a 128-atom cell, so that the error in the energy difference between the two structures is less than our target accuracy of 30 eV/atom.

### 3.2 Production results

In Fig. 4 we display DMC energies as a function of volume for MgO in the NaCl structure. The length of these simulations was typically 6000 steps, resulting in a statistical error bar of less than 10 meV/atom. These energy points were then used to fit the parameters of the Birch-Murnaghan equation of state [53]:

$$E = E_0 + \frac{3}{2}V_0B_0 \left[ \frac{3}{4}(1 + 2\xi) \left(\frac{V_0}{V}\right)^{4/3} - \frac{\xi}{2} \left(\frac{V_0}{V}\right)^2 - \frac{3}{2}(1 + \xi) \left(\frac{V_0}{V}\right)^{2/3} + \frac{1}{2} \left(\xi + \frac{3}{2}\right) \right], \quad (2)$$

where  $\xi = (3 - 3B'_0/4)$ ,  $V_0$  is the equilibrium volume,  $B_0$  is the zero-pressure bulk modulus,  $B'_0$  is its derivative with respect to pressure at zero pressure, and  $E_0$  is the energy at the minimum. The fitted curve is also reported on the same Figure. The values of the fitted parameters are reported in Table 1 together with other theoretical results and experimental data. A comparison of the QMC results with experimental values shows that our calculated lattice parameter of  $a_0 = 4.098 \text{ \AA}$  is smaller than the measured value of  $a_0 = 4.213 \text{ \AA}$  [34], and our bulk modulus  $B_0 = 183 \text{ GPa}$  is greater than the measured value  $B_0 = 160 \pm 2 \text{ GPa}$  [34]. However, two kinds of corrections need to be made. It is known from earlier DFT calculations [35] that room temperature thermal pressure due to lattice vibrations increases  $a_0$  by 0.03  $\text{\AA}$  and decreases  $B_0$  by 10 GPa. We should also correct for pseudopotential errors. To estimate these, we have compared the predictions of pseudopotential and all-electron HF calculations using the CRYSTAL [36] code (see Table 1). This shows that the pseudopotentials we have used underestimate  $a_0$  by 0.10  $\text{\AA}$  and overestimate  $B_0$  by 15 GPa. Combining these two corrections, our revised QMC values are  $a_0 = 4.23 \text{ \AA}$  and  $B_0 = 158 \text{ GPa}$ , which are very close to the experimental values.

In Fig. 5 we report the DMC energy for MgO in the NaCl and the CsCl structures evaluated for volumes corresponding to roughly one half of the zero pressure equilibrium volume, which is the region of volumes in which the transition occurs. These energy points have also been fitted to the Birch-Murnaghan equation of state, which we have then used to compute the enthalpies of the two structures, which are displayed in the upper part of Fig. 6, from which we infer a transition pressure of about 597 GPa. We note that the slopes of the two curves are very similar, and that an error of about 1 meV/atom in the relative enthalpy results in an error in the transition pressure of about 1 GPa. We do not expect our DMC results to be more accurate than about 20 meV/atom, so our computed transition pressure should be considered to have an error bar of about 20 GPa. For comparison, we also report in the lower part of Fig. 6 the enthalpy evaluated with DFT-LDA and the same pseudopotentials, from which we deduce a transition pressure of 569 GPa.

## 4 Discussion and conclusions

An important conclusion from this work is that it is technically feasible to carry out diffusion Monte Carlo calculations on MgO at the level of accuracy required to compute quantities such as the equilibrium lattice constant, the bulk modulus, and the B1-B2 transition pressure. As we mentioned in the Introduction, this is a non-trivial conclusion, because DMC calculations succeed in practice only if the many-body trial wave function is sufficiently close to the true ground state wave function. Even though MgO should be a favourable oxide in this respect, it was still essential to pay careful attention to the accurate representation of the single-electron orbitals in order to bring statistical fluctuations under control.

We have shown that, provided corrections are made for thermal effects and errors due to imperfections of our pseudopotentials, the QMC predictions of lattice parameter  $a_0$  and bulk modulus  $B_0$  agree with experimental values to within  $\sim 0.5\%$  for  $a_0$  and to within experimental error ( $\sim 2\%$ ) for  $B_0$ . In future work, there should be scope for further improvement in the pseudopotentials. It is interesting to note that our QMC prediction for  $a_0$  is almost identical to the HF prediction with the same pseudopotentials. This might seem to suggest that correlation effects are negligible in MgO. However, this is certainly not the case. The correlation energy is at least the difference between the HF and the QMC total energies. We find that for the rock-salt structure near the equilibrium volume, this difference is  $\sim 4.5$  eV/atom. The close agreement between the HF and QMC lattice parameters therefore indicates that this rather large correlation energy depends only weakly on volume. Our QMC value of  $597 \pm 20$  GPa for the B1-B2 transition pressure supports the most recent DFT predictions of a pressure in the region of  $\sim 500$  GPa, which is beyond the region of geophysical interest (the pressure at the core-mantle boundary of the Earth is 135 GPa). The detailed value we have found may suffer from a pseudopotential error, but at present we are unable to quantify this.

With these encouraging results for MgO, we believe that there are now good prospects for extending QMC methods to studying the more challenging problems involving MgO mentioned in the introduction, and to studies of transition metal oxides. LDA (and generalised gradient approximation) calculations are unsuitable for transition metal oxides because they lead to an incorrect filling of the energy levels. Unrestricted HF and B3LYP orbitals have already been used with some success in DMC studies of transition metal oxides [17, 18], and one might also consider using LDA+U or SIC (self-interaction corrected) DFT orbitals. Towler and Needs [52] found that unrestricted HF orbitals gave a lower energy than B3LYP orbitals for NiO. Transition metal oxides are clearly a case where it would be useful to optimise the orbitals in the presence of the Jastrow factor.

## References

- [1] W. M. C. Foulkes, L. Mitaš, R. J. Needs, and G. Rajagopal, *Rev. Mod. Phys.* **73**, 33 (2001).
- [2] W.-K. Leung, R. J. Needs, G. Rajagopal, S. Itoh, and S. Ihara, *Phys. Rev. Lett.* **83**, 2351 (1999).
- [3] R. Q. Hood, P. R. C. Kent, R. J. Needs, and P. R. Briddon, *Phys. Rev. Lett.* **91**, 076403 (2003).
- [4] S. B. Healy, C. Filippi, P. Kratzer, E. Penev, and M. Scheffler, *Phys. Rev. Lett.* **87**, 016105 (2001).
- [5] C. Filippi, S. B. Healy, P. Kratzer, E. Pehlke, and M. Scheffler, *Phys. Rev. Lett.* **89**, 166102 (2002).
- [6] A. J. Williamson, J. C. Grossman, R. Q. Hood, A. Puzder, and G. Galli, *Phys. Rev. Lett.* **89**, 196803 (2002).
- [7] D. M. Ceperley and B. J. Alder, *Phys. Rev. Lett.* **45**, 566 (1980).
- [8] J. B. Anderson, *J. Chem. Phys.* **65**, 4121 (1976).
- [9] A. R. Oganov, M. J. Gillan, and G. D. Price, *J. Chem. Phys.* **118**, 10174 (2003).
- [10] A. R. Oganov and P. I. Dorogokupets, *Phys. Rev. B* **67**, 224110 (2003).

- [11] C. Zhang and P. J. D. Lindan, *J. Chem. Phys.* **119**, 9183 (2003).
- [12] J. L. Gavartin, P. V. Suchko and A. L. Shluger, *Phys. Rev. B* **67**, 035108 (2003).
- [13] A. Zerr and R. Boehler, *Nature* **371**, 506 (1994).
- [14] R. E. Cohen and Z. Gong, *Phys. Rev. B* **50**, 12301 (1994).
- [15] L. Vočadlo and G. D. Price, *Phys. Chem. Miner.* **23**, 42 (1996).
- [16] A. Strachan, R. Çağın, and W. A. Goddard III, *Phys. Rev. B* **60**, 15084 (1999).
- [17] R. J. Needs and M. D. Towler, *Int. J. Mod. Phys. B* **17**, 5425 (2003).
- [18] J.-W. Lee, L. Mitaš, and L. K. Wagner, unpublished.
- [19] R. J. Needs, M. D. Towler, N. D. Drummond, and P. R. C. Kent, ‘CASINO Version 1.7 User Manual’, University of Cambridge, Cambridge (2004).
- [20] A. J. Williamson, S. D. Kenny, G. Rajagopal, A. J. James, R. J. Needs, L. M. Fraser, W. M. C. Foulkes, and P. Maccallum, *Phys. Rev. B* **53**, 9640 (1996).
- [21] C. J. Umrigar, K. G. Wilson, and J. W. Wilkins, *Phys. Rev. Lett.* **60**, 1719 (1988).
- [22] P. R. C. Kent, R. J. Needs, and G. Rajagopal, *Phys. Rev. B* **59**, 12344 (1999).
- [23] J. R. Trail and R. J. Needs, to appear in *J. Chem. Phys.*
- [24] C. W. Greeff and W. A. Lester, Jr., *J. Chem. Phys.* **109**, 1607 (1998).
- [25] P. R. Kent, R. Q. Hood, M. D. Towler, R. J. Needs, and G. Rajagopal, *Phys. Rev. B* **57**, 15293 (1998).
- [26] S. Baroni, A. Dal Corso, S. de Gironcoli, and P. Giannozzi, <http://www.pwscf.org>.
- [27] D. Alfè and M. J. Gillan, *Phys. Rev. B* **70**, 161101(R) (2004).
- [28] L. M. Fraser, W. M. C. Foulkes, G. Rajagopal, R. J. Needs, S. D. Kenny, and A. J. Williamson, *Phys. Rev. B* **53**, 1814 (1996).
- [29] A. J. Williamson, G. Rajagopal, R. J. Needs, L. M. Fraser, W. M. C. Foulkes, Y. Wang, and M.-Y. Chou, *Phys. Rev. B* **55**, 4851 (1997).
- [30] P. R. Kent, R. Q. Hood, A. J. Williamson, R. J. Needs, W. M. C. Foulkes, and G. Rajagopal, *Phys. Rev. B* **59**, 1917 (1999).
- [31] R. Maezono, M. D. Towler, Y. Lee, and R. J. Needs, *Phys. Rev. B* **68**, 165103 (2003).
- [32] C. Filippi and S. Fahy, *J. Chem. Phys.* **112**, 3523 (2000).
- [33] A. J. Williamson, R. Q. Hood, R. J. Needs, and G. Rajagopal, *Phys. Rev. B* **57**, 12140 (1998).
- [34] Y. Fei, *Am. Mineral.* **84**, 272 (1999).
- [35] B. B. Karki, R. M. Wentzcovitch, S. de Gironcoli, and S. Baroni, *Phys. Rev. B* **61**, 8793 (2000).
- [36] V. R. Saunders, R. Dovesi, C. Roetti, M. Causà, N. M. Harrison, R. Orlando, and C. M. Zicovich-Wilson, *CRYSTAL98 User’s Manual* (University of Torino, Torino, 1998).
- [37] R. W. G. Wyckoff, *Crystal Structures*, Vol. 1, Second edition, Interscience Publishers, New York (1963).
- [38] S. Speziale, C.-S. Zha, T. S. Duffy, R. J. Hemley, and H.-K. Mao, *J. Geophys. Res. B* **106**, 515 (2001).

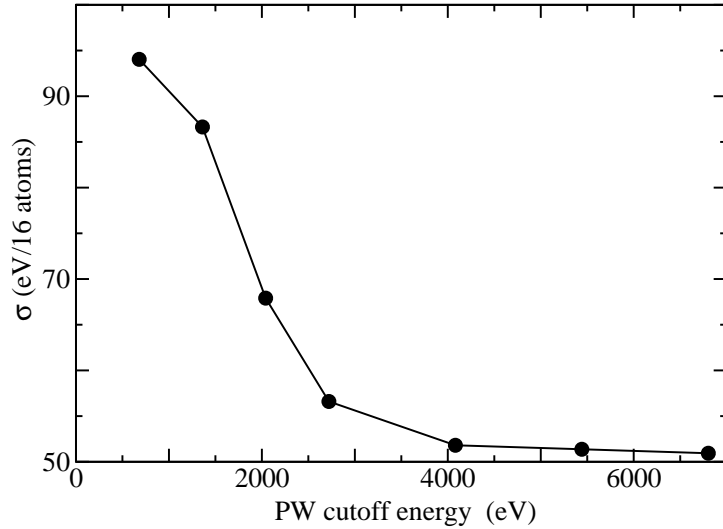


Figure 1: The standard error in the energy,  $\sigma$ , for runs of the same length, calculated within VMC without a Jastrow factor, as a function of the plane-wave cut-off energy, for a 16-atom cell of MgO in the rock-salt structure with a lattice parameter of 4.17 Å.

- [39] O. L. Anderson and P. Andreatch, *J. Am. Ceram. Soc.* **49**, 404 (1966).
- [40] H.-K. Mao and P. Bell, *J. Geophys. Res.* **84**, 5433 (1979).
- [41] T. S. Duffy, R. J. Hemley, and H.-K. Mao, *Phys. Rev. Lett.* **74**, 1371 (1995).
- [42] M. I. McCarthy and N. M. Harrison, *Phys. Rev. B* **49**, 8574 (1994).
- [43] F. Marinelli and A. Lichanot, *Chem. Phys. Lett.* **367**, 430 (2003).
- [44] M. Causà, R. Dovesi, C. Pisani, and C. Roetti, *Phys. Rev. B* **33**, 1308 (1986).
- [45] B. B. Karki, L. Stixrude, S. J. Clark, M. C. Warren, G. J. Ackland, and J. Crain, *Am. Mineral.* **82**, 51 (1997).
- [46] M. J. Mehl, R. E. Cohen, and H. Krakauer, *J. Geophys. Res.* **93**, 8009 (1988).
- [47] J. E. Jaffe, J. A. Snyder, Z. Lin, and A. C. Hess, *Phys. Rev. B* **62**, 1660 (2000).
- [48] K. J. Chang and M. L. Cohen, *Phys. Rev. B* **30**, 4774 (1984).
- [49] M.-P. Habas, R. Dovesi, and A. Lichanot, *J. Phys: Condens. Matter* **10**, 6897 (1998).
- [50] N. D. Drummond and G. J. Ackland, *Phys. Rev. B* **65**, 184104 (2002).
- [51] T. Tsuchiya and K. Kawamura, *J. Chem. Phys.* **114**, 10086 (2001).
- [52] M. D. Towler and R. J. Needs, unpublished.
- [53] F. Birch, *Phys. Rev.* **71**, 809 (1947).



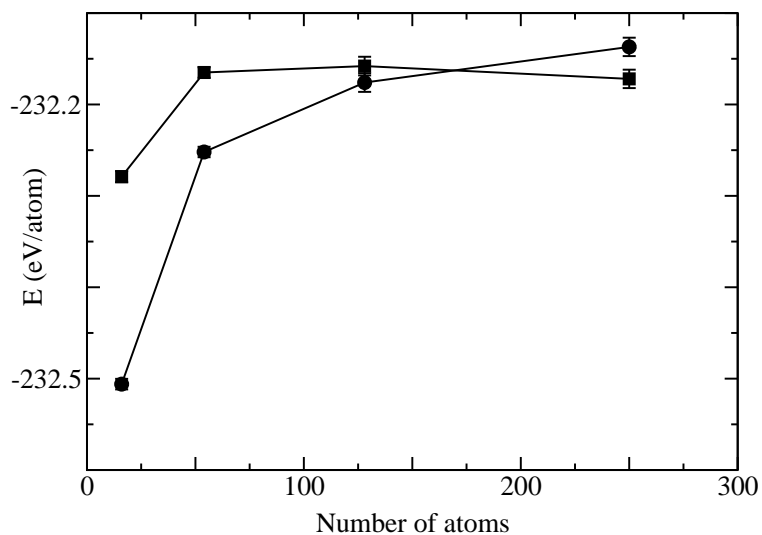


Figure 2: The VMC energy per atom for MgO in the rock-salt structure with a volume per atom of  $9.06 \text{ \AA}^3$  as a function of the number of atoms in the repeating cell, using both the Ewald interaction (circle) and the MPC interaction (squares).

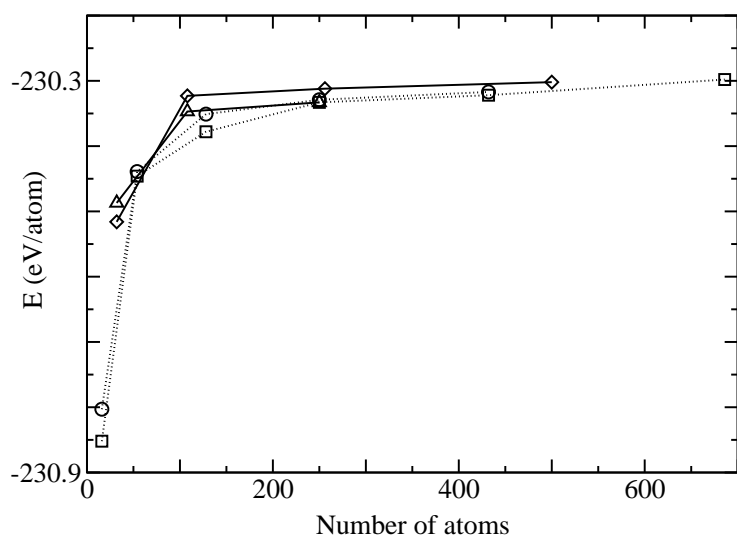


Figure 3: The VMC energy per atom for MgO in the CsCl structure with a volume per atom of  $8.77 \text{ \AA}^3$  as a function of the number of atoms in the repeating cell, calculated using the Ewald interaction. Squares and circles: simple cubic cell with  $\Gamma$ -point and zone-boundary sampling, respectively; diamonds and triangles: fcc cell with  $\Gamma$ -point and zone-boundary sampling (see text for wavevector used in zone-boundary sampling). The lines are guides to the eye.

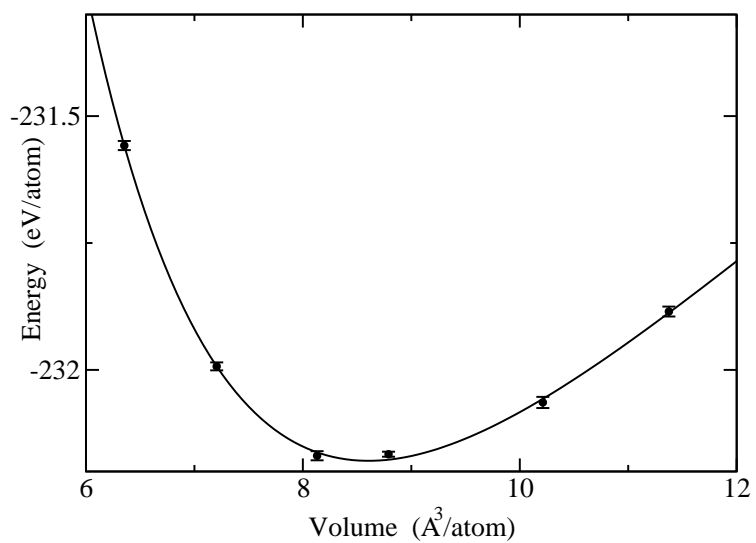


Figure 4: The DMC energy per atom as function of volume for MgO in the NaCl structure.

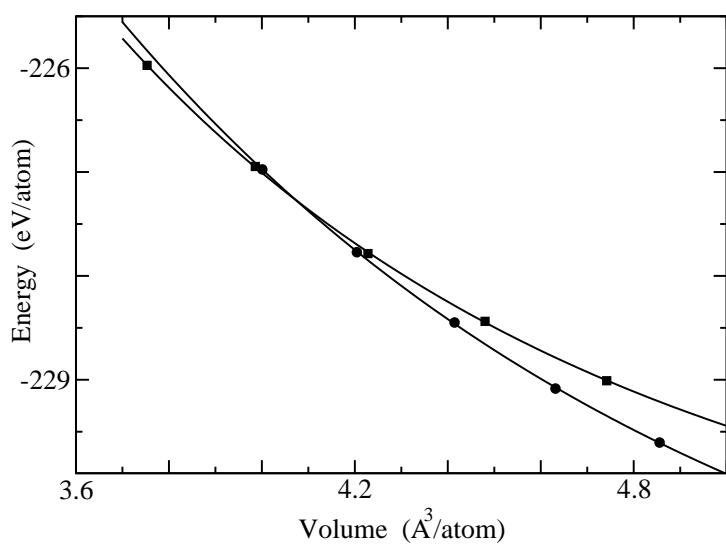


Figure 5: The DMC energy per atom for the NaCl structure (circles) and the CsCl structure (squares) of MgO as a function of volume in the region of the B1-B2 phase transition.

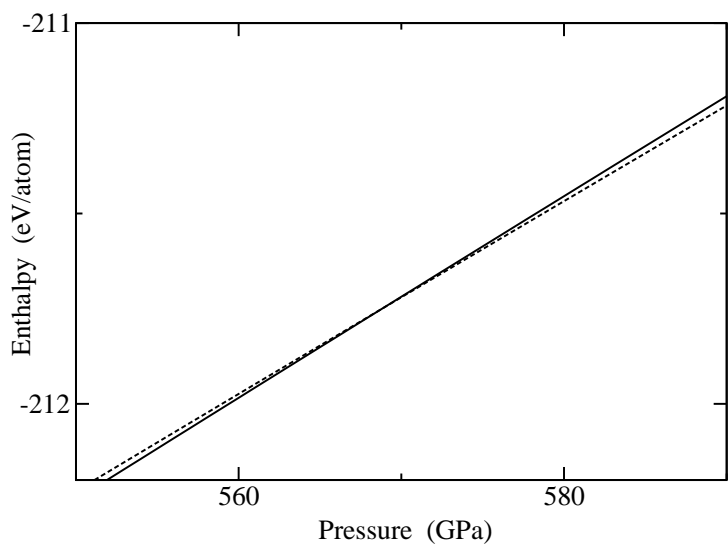
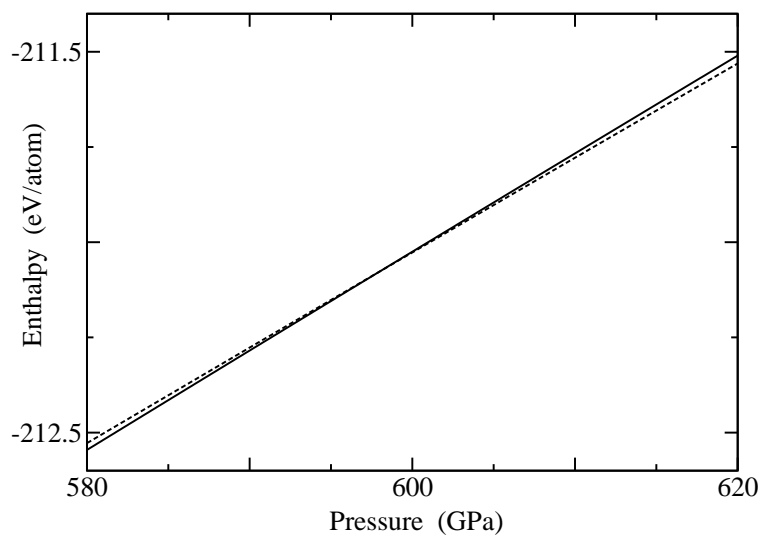


Figure 6: The enthalpy per atom of the NaCl and CsCl (dashed line) structures of MgO as a function of pressure. Top picture: fit to the DMC data; bottom picture: fit to the DFT-LDA data.

	$a_0$ (Å)				$B_0$ (GPa)			$P_{\text{tr}}(\text{B1-B2})$ (GPa)	
Experiments	4.213 <sup>a</sup>	4.211 <sup>b</sup>	4.212 <sup>c</sup>	4.19 <sup>d</sup>	160±2 <sup>a</sup>	160.2 <sup>c</sup>	156 <sup>e</sup>	164.6 <sup>d</sup>	> 227 <sup>f</sup>
QMC	4.098 <sup>g</sup>				183 <sup>g</sup>			597±20 <sup>g</sup>	
HF-PP	4.089 <sup>g</sup>				196 <sup>g</sup>				
HF-AE	4.195 <sup>g,h</sup>	4.200 <sup>i</sup>			181 <sup>g,h</sup>	182 <sup>i</sup>			
HF-LCAO	4.201 <sup>j</sup>	4.191 <sup>q</sup>			186 <sup>j</sup>	182 <sup>q</sup>		220 <sup>j</sup> 712 <sup>q</sup>	
B3LYP	4.230 <sup>i</sup>				162 <sup>i</sup>				
DFT-LDA	4.160 <sup>i</sup>	4.240 <sup>k</sup>	4.194(4.222) <sup>l</sup>		198 <sup>i</sup>	172.6 <sup>k</sup>	169(159) <sup>l</sup>		490 <sup>k</sup> 451 <sup>m</sup> 510 <sup>n</sup>
	4.25 <sup>m</sup>	4.167 <sup>n</sup>	4.163 <sup>o</sup>	4.191 <sup>p</sup> 4.160 <sup>q</sup>	159.7 <sup>m</sup>	172 <sup>n</sup>	185.9 <sup>o</sup>	146 <sup>p</sup> 181 <sup>q</sup>	515 <sup>o</sup> 1050 <sup>p</sup> 512 <sup>q</sup>
DFT-GGA	4.273 <sup>q</sup>	4.243 <sup>q</sup>	4.247 <sup>o</sup>	4.244 <sup>i</sup>	153 <sup>q</sup>	160 <sup>q</sup>	159 <sup>q</sup>	169.1 <sup>o</sup> 157 <sup>i</sup>	478 <sup>q</sup> 428 <sup>q</sup> 418 <sup>q</sup> 515 <sup>o</sup>
	4.253 <sup>r</sup>	4.259 <sup>s</sup>	4.218 <sup>u</sup>	4.259 <sup>v</sup>	150.6 <sup>r</sup>	161.5 <sup>u</sup>	160 <sup>v</sup>		509 <sup>r</sup> 664 <sup>s</sup> 400 <sup>u</sup>

<sup>a</sup> Ref. [34]

<sup>b</sup> Ref. [37]

<sup>c</sup> Ref. [38]

<sup>d</sup> Ref. [39]

<sup>e</sup> Ref. [40]

<sup>f</sup> Ref. [41]

<sup>g</sup> This work.

<sup>h</sup> Ref. [42]

<sup>i</sup> Ref. [43]

<sup>j</sup> Ref. [44]

<sup>k</sup> Ref. [9]

<sup>l</sup> Ref. [35]; values in parenthesis include zero point motion and room temperature effects.

<sup>m</sup> Ref. [45]

<sup>n</sup> Ref. [46]

<sup>o</sup> Ref. [47]

<sup>p</sup> Ref. [48]

<sup>q</sup> Ref. [49]

<sup>r</sup> Ref. [10]

<sup>s</sup> Ref. [50]

<sup>u</sup> Ref. [16]

<sup>v</sup> Ref. [51]

Table 1: DFT and HF values for the lattice constant and bulk modulus of the NaCl phase of MgO, and the equilibrium pressure for the B1-B2 transition. See the original references for details.

Number of atoms	Energy (eV/atom)	
	NaCl	CsCl
32		-227.143(6)
54	-227.971(4)	
108		-226.914(4)
128	-227.846(3)	
250	-227.806(5)	
256		-226.867(5)
432	-227.794(7)	
500		-226.866 (9)

Table 2: VMC energies for MgO in the NaCl and CsCl structures at volumes per atom 4.41 and 4.23 Å<sup>3</sup> respectively, as a function of the number of atoms in the repeating cell.